The Laryngoscope

Preclinical Assessment of Resorbable Silk Splints for the Treatment of Pediatric Tracheomalacia

Meghan McGill, BS; Nikhila Raol, MD, MPH; Kevin S. Gipson, MD, MS; Sarah N. Bowe, MD; Jackson Fulk-Logan, BS; Anahita Nourmahnad, BS; Joon Yong Chung, BS; Michael J. Whalen, MD; David L. Kaplan, PhD; Christopher J. Hartnick, MD

Objective: Tracheomalacia is characterized by weakness of the tracheal wall resulting in dynamic airway collapse during respiration; severe cases often require surgical intervention. Off-label external splinting with degradable implants has been reported in humans; however, there remains a need to develop splints with tunable mechanical properties and degradation profiles for the pediatric population. The objective of this pilot study is to assess the safety and efficacy of silk fibroin-based splints in a clinically relevant preclinical model of tracheomalacia.

Methods: Silk splints were evaluated in a surgically induced model of severe tracheomalacia in N = 3 New Zealand white rabbits for 17, 24, and 31 days. An image-based assay was developed to quantify the dynamic change in airway area during spontaneous respiration, and histopathology was used to study the surrounding tissue response.

Results: The average change in area in the native trachea was 23% during spontaneous respiration; surgically induced tracheomalacia resulted in a significant increase to 86% ($P < 0.001$). The average change in airway area after splint placement was reduced at all terminal time points (17, 24, and 31 days postimplantation), indicating a clinical improvement, and was not statistically different than the native trachea. Histopathology showed a localized inflammatory reaction characterized by neutrophils, eosinophils, and mononuclear cells, with early signs suggestive of fibrosis at the splint and tissue interface.

Conclusion: This pilot study indicates that silk fibroin splints are well tolerated and efficacious in a rabbit model of severe tracheomalacia, with marked reduction in airway collapse following implantation and good tolerability over the studied time course.

Key Words: Tracheomalacia, resorbable splint, airway obstruction, silk fibroin, preclinical.

Level of Evidence: NA.

***Laryngoscope*, 00:1–6, 2018**

INTRODUCTION

Tracheomalacia is characterized by weakness of the tracheal wall, resulting in dynamic airway collapse during respiration.[1] The incidence of primary tracheomalacia in children is estimated to be at least one in 2,100[2]; symptoms range from chronic cough and wheezing in milder cases to life-threatening airway occlusion in more severe cases.[3] Conservative medical treatment is preferred for mild malacia, with the expectation that the tracheal wall will strengthen on its own and symptoms will improve by 2 years of age.[4] However, severe tracheomalacia accounts for approximately half of all cases[5] and often requires surgical intervention.[1]

Established surgical procedures for severe tracheomalacia include aortopexy, resection, and stenting.[1] Aortopexy relieves vascular compression on the trachea and has a high success rate and low morbidity.[6] However, the procedure has limited utility where long or multiple segments of the trachea are affected, or where the source of compression is not a nearby vessel.[5] Resection of the affected airway segment followed by anastomosis is another option to relieve symptoms of severe tracheomalacia. This technique is also limited to treating short segments of the airway, and there is a risk of tension on the anastomosis site.[7] Internal stenting with silicone or metal stents offers a less invasive procedure and shorter recover time; however, formation of granulation tissue, stent migration, and difficult removal are common complications.[1,8]

Resorbable splints that can be externally affixed to the airway have emerged as a promising option for treating pediatric patients with severe tracheomalacia and aim to overcome the limitations associated with internal stents.[9] In order to be effective, the splint must have sufficient radial strength to prevent airway collapse, degrade over a clinically appropriate time period into innocuous products, and be easy to affix to the tracheal wall.

From the Department of Biomedical Engineering, Tufts University (M.MCG., J.F-L., D.L.K.), Medford; the Department of Otolaryngology–Head and Neck Surgery, Massachusetts Eye and Ear Infirmary (N.R., S.N.B., A.N., C. J.H.); Department of Pediatrics, Division of Pediatric Pulmonology (K.S.G.); the Department of Pediatrics, Massachusetts General Hospital (J.Y.C., M.J.W.); the Harvard Medical School (A.N.), Boston, Massachusetts; and the Department of Otolaryngology–Head and Neck Surgery (N.R.), Emory University School of Medicine, Atlanta, Georgia, U.S.A

Institution where work was performed: Massachusetts Eye and Ear Infirmary, Boston, Massachusetts, U.S.A.

Editor's Note: This Manuscript was accepted for publication on August 3, 2018.

This study was supported by the National Institutes of Health (NIH) R01AR068048. The authors have no other funding, financial relationships, or conflicts of interest to disclose.

Send correspondence to Christopher J. Hartnick, MD, Massachusetts Eye & Ear Infirmary, 243 Charles St, Boston MA 02114. E-mail: christopher_hartnick@meei.harvard.edu

DOI: 10.1002/lary.27540

External splints and fixation plates from nondegradable materials such as polytetrafluoroethylene[10] and polyetherketoneketone,[11] as well as degradable materials including polycaprolactone,[12,13] polydioxanone,[14,15] and (D,L-lactide-co-glycolide),[16–19] have been reported in both preclinical and human use. However, there remains a need to develop splints with modifiable mechanical properties and degradation profiles. Silk fibroin (SF) is a naturally derived polymer from the cocoons of *Bombyx mori* silkworms that exhibits excellent strength and resiliency, tunable degradation, and a mild immune response in vivo.[20] Due to its remarkable properties rivaling those of the best synthetic polymers, silk has been utilized in implantable devices[21–23] and is a promising material for resorbable tracheal splints.

The objective of the present study was to assess the safety and efficacy of silk-based splints in a clinically relevant in vivo model of tracheomalacia. Tracheal collapse was studied by quantifying changes in airway area using a bronchoscopy imaging method 1) before injury (control), 2) after injury, 3) after splint placement, and 4) at the time of explant. The surrounding tissue response was assessed by histological analysis. This pilot study reveals a promising opportunity for external resorbable splints fabricated from silk to treat severe tracheomalacia.

MATERIALS AND METHODS

Splint Fabrication and in vitro Degradation

Splints were fabricated from reconstituted SF in a two-step process. First, 150 mg/mL aqueous SF purified from native *Bombyx mori* cocoons was cast into molds and lyophilized to form solid 180° constructs (freezing: 0.5°C/minute to 40°C, primary drying: −20°C at 100 millitors (mTorr), secondary drying: 4°C at 100 mTorr). The splints were then immersed in methanol for 1 hour to render them insoluble. Next, 150 mg/mL SF was spin cast onto the exterior of the splint to a thickness of approximately 1 mm, and the coated splints were immersed in methanol for 60 minutes. The resulting splints were sterilized with ethylene oxide and allowed to off-gas for at least 72 hours.

Mechanical properties were assessed with a uniaxial mechanical tester (model 3366, Instron (model 3366, Instron, Norwood, MA) as the splints were degraded in a protease solution (1.0 U/mL Protease XIV in phosphate buffered saline [PBS], Sigma-Aldrich, St. Louis, MO) at 37°C to mimic in vivo degradation. Mechanical testing of the hydrated splints comprised of a cyclic compression test (0 to 30%) with five cycles at a rate of 1.0 mm/minute; the maximum force was extracted from the peak force in the final cycle (N = 4 samples per time point). Degradation was determined by the change in mass of the dried sample from the dry mass at day 0. Samples were imaged under scanning electron microscopy (SEM) to observe the surface topography as they degraded.

Tracheomalacia Model and Study Design

We sought to validate the external tracheal splint design in a New Zealand white rabbit model in a small pilot study. This work was approved by the Massachusetts Eye and Ear Institute (MEEI) Institutional Animal Care and Use Committee (protocol #15-006). The rabbit model was selected for its tracheal anatomy and intrinsic dynamics, which are comparable to those of the human infant. Three male rabbits (weights approximately 3 kg) were used in this study, with the male gender selected for the relative paucity of redundant skin overlying the neck (*dewlap*) compared to females. Preanesthetic sedation and analgesia was achieved by the intramuscular administration of ketamine (25 mg/kg) and xylazine (3.75 mg/kg). Once sedated, the ear was prepped and a fentanyl (12 mcg/hour) transdermal patch was applied for postoperative analgesia. Then, a catheter was placed in the auricular vein, and buprenorphine (0.05 mg/kg) was given intravenously (IV) once. Maintenance IV fluids were initiated, and the rabbit was placed supine on a water-circulating warming pad. Pulse oximetry was applied, and blood oxygen saturation (SpO_2) and heart rate was monitored continuously throughout the procedure. A laryngeal mask airway (LMA) was inserted, and position checked by "fogging" of the tube with respirations and observation of symmetric chest rise. Anesthesia was then induced with isoflurane (1%–5%), and supplemental oxygen was bled into the ventilator circuit and titrated as necessary to maintain $SpO_2 > 92\%$. End-tidal CO_2 ($EtCO_2$) monitoring was continuous throughout the procedure.

The neck was prepared by removing overlying fur and sterilizing with betadine swabs. A flexible bronchoscope (Karl Storz 11101rp2 flexible rhino-pharyngo laryngoscope, OD 3.5 mm; Tuttlingen, Germany) was then passed into the ventilator circuit via a port, then through the LMA and past the vocal folds into the trachea. The position of the bronchoscope was noted by observing the depth markings on the scope sleeve and the light at the distal tip of the bronchoscope through the overlying soft tissue of the neck. Video of at least three spontaneous breath cycles, defined as a full inspiration and expiration, was recorded for subsequent airway dynamics assay described below, and then the bronchoscope was withdrawn. A cervical incision was made over the airway extending superiorly from the level of the cricoid cartilage and inferiorly over the upper cervical trachea. The incision was carried down through the skin and subcutaneous tissues to the level of the strap musculature, which were divided in the midline and retracted laterally to expose the underlying trachea. The surgical technique for inducing tracheomalacia was developed by Dr. Kishore Sandu (oral communication, 2016). Using a Beaver mini-blade, the anterior aspect of four tracheal rings overlying the site of the initial airway dynamics assay were meticulously dissected away from the underlying tracheal mucosa and submucosa to approximately the point of the trachea-esophageal grove (Fig. 1). At this time, the rabbit was given positive pressure breaths via the ventilator circuit to check for air leak through the mucosa/submucosa that may have been introduced during tracheal ring removal. Uniformly, at this step in the protocol no air leak was observed for the three rabbits.

The bronchoscope was then inserted to the same depth using the printed ruler on the sheath, and a video recording of at least three spontaneous breath cycles was again made. The bronchoscope was withdrawn, and the bioresorbable tracheal splint, previously hydrated in sterile PBS, was overlain on the denuded area of trachea. The splint was sutured to the tracheal mucosa at the lateral aspects of the splint with 4-0 Monocryl (Somerville, NJ) suture (Fig. 1). The overlying musculature was then reapproximated with 3-0 Vicryl (Ethicon) suture. The skin was closed in a multi-layer fashion with 3-0 Vicryl buried deep dermal sutures and running 5-0 fast absorbing plain gut. Finally, a rubber band drain was placed at the distal aspect of the incision. The rabbit was again given positive-pressure breaths to observe for air leak through the mucosa/submucosa, which commonly occurred following placement of the sutures. The air, however, easily escaped via the rubber band drain following cessation of positive-pressure ventilation. Following full closure of the surgical incision the bronchoscope was again placed through the LMA to the predetermined depth; a third video of three spontaneous breath cycles was recorded; and the scope was withdrawn.

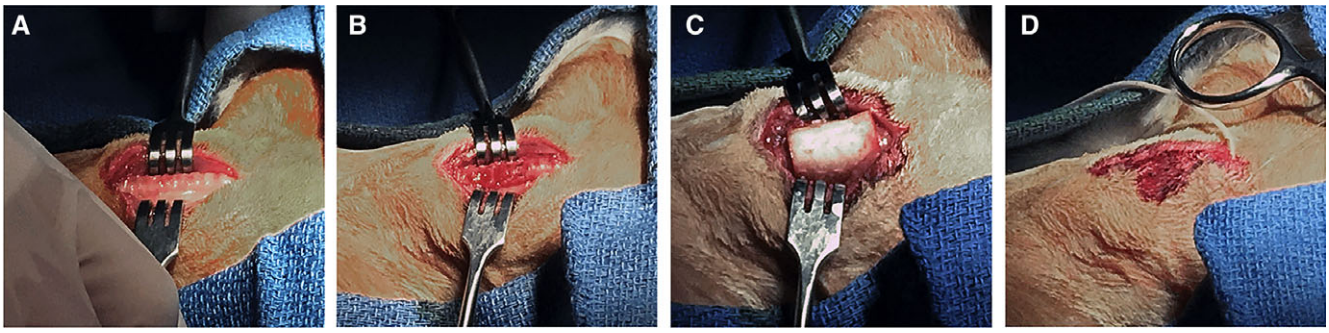

Fig. 1. Tracheal ring resection and splint implantation. (A) The trachea is exposed via a vertical incision; and the overlying skin, muscle, and fascia is gently retracted laterally. (B) Under sterile technique, the tracheal rings are carefully dissected from the mucosa to induce airway malacia. (C) The splint is sutured into place. (D) The surgical incision is closed with a rubber band drain left in place. [Color figure can be viewed in the online issue, which is available at www.laryngoscope.com.]

The rabbit was recovered in the operating room and returned to the animal care facility (ACF) when righting reflex reemerged. Each rabbit received twice-daily subcutaneous boluses of normal saline for the first 72 hours postoperatively and was otherwise observed and cared for per protocol in the ACF until the end of the study period. At either postoperative day 17, 24, or 31, respectively, each rabbit was brought back to the operating room. Preoperative sedation, analgesia, and operative anesthesia were achieved through use of ketamine, xylazine, and isoflurane, as above. The rabbit was allowed to breathe spontaneously on a ventilator circuit via LMA. A bronchoscope was passed through the LMA to the level of the depth markings noted at the time of splint placement, with additional confirmation by palpation of the splint and observation of the airway movement on the bronchoscope. A video recording of three breath cycles was obtained. Then, the rabbit was euthanized using Fatal-Plus solution (pentobarbital sodium, active ingredient), with completed euthanasia confirmed via pulse oximetry and cardiac auscultation. The neck was then incised, and the trachea was then resected en bloc with the splint in place and placed in paraformaldehyde (4% in PBS) for fixation. This tissue was then processed in paraffin section and stained with hematoxylin and eosin. Photomicrosopy of relevant aspects was obtained and is presented below.

Preclinical Outcomes

Following tracheal splint implantation, the rabbits were observed and maintained per ACF guidelines, and monitored for respiratory distress, stridor, weight loss, and other objective signs of postoperative complications.

We used an image-based assay to quantify the change in airway area during spontaneous respiration, and therefore assess the degree of tracheomalacia in our model. Previous work has established dynamic computed tomography scans and similar combination of image analysis to calculate the airway area and collapse as a method to diagnose tracheomalacia.[24,25] From each bronchoscopic video recording, still images of the maximum and minimum airway lumen were generated for three breath cycles (Fig. 2). These images were then adjusted to maximize the contrast between the lumen and tracheal wall. The resulting images were then randomized and provided to a blinded analyst. The analyst determined the area of the airway lumen by tracing the wall of the lumen in ImageJ, which outputs an area in pixels. Using these measurements, the percent change in airway area was calculated in triplicate for each rabbit at each operative stage using the following equation:

$$[(Lumen\ area_{max} - Lumen\ area_{min}) \div Lumean\ area_{max}] \times 100 = Change\ in\ area\ (\%).$$

The change in area (%) is reported as an average of N = 3 breath cycles for each animal at the following operative stages: in the native trachea (control), immediately following surgical inducement of tracheomalacia, immediately after splint implantation, and at the time of explantation (day 17, 24, or 31). Statistical

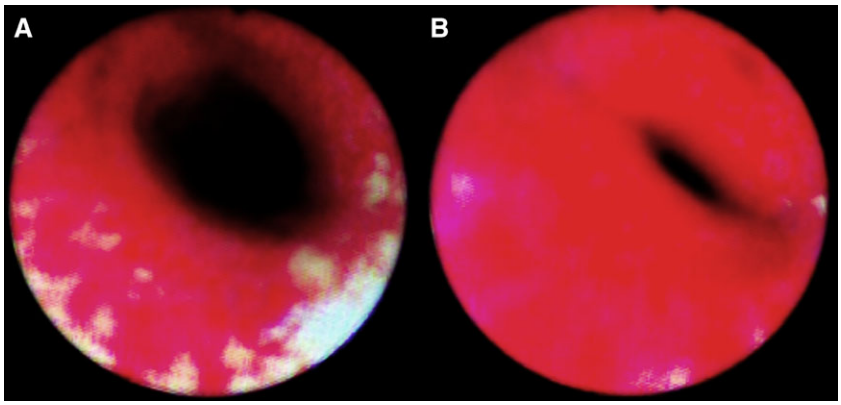

Fig. 2. An example of the surgically induced tracheomalacia in a rabbit airway prior to implantation of the bioresorbable SF splint. (A) Maximal lumen size with tidal expiration, and (B) minimum lumen size during spontaneous inhalation. Under the described quantitative image-based assay, this represents a calculated 93% reduction in airway caliber. [Color figure can be viewed in the online issue, which is available at www.laryngoscope.com.]

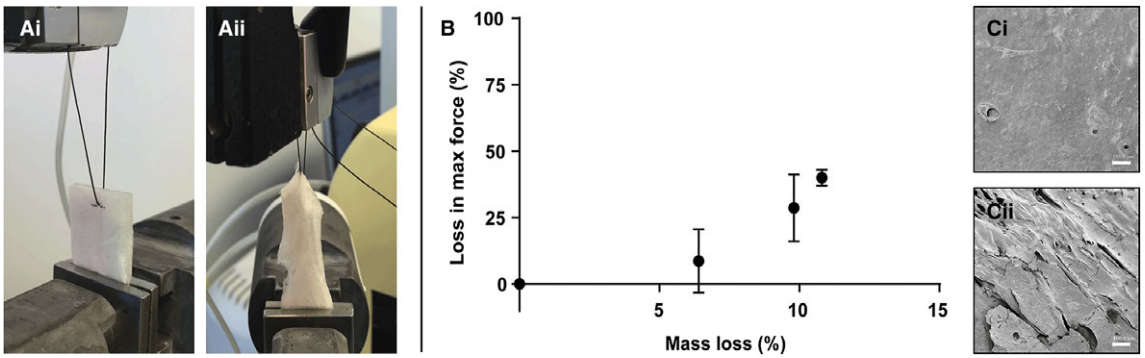

Fig. 3. Suture inserted into a sample of SF splint (Ai) and stressed to failure (Aii) demonstrating that a suture can be inserted and resist a substantial force (1.8 ± 0.5 N, N = 3). Loss in maximum force (%) versus loss in mass (%) of SF splints incubated in a protease solution at 37°C over 6 weeks to mimic in vivo degradation (B). Maximum force was obtained from cyclic compression testing and is reported as an average and standard deviation of N = 4 samples. Scanning electron microscopy images corresponding to a mass loss of 0 (Ci) and 10% (Cii) show evidence of degradation. Scale bar 100 μm.SF = silk fibroin. [Color figure can be viewed in the online issue, which is available at www.laryngoscope.com.]

comparison was determined by one-way analysis of variance with Tukey post hoc test, with significance defined as $P < 0.05$.

RESULTS

Splint Fabrication and Mechanics

The two-step fabrication process comprising of freeze-drying and spin coating resulted in SF splints that were both flexible and stiff. Freeze-drying yielded a porous and flexible splint that could be contoured to fit the external tracheal wall, cut to size on the operating table if needed, and hold a suture passed through anywhere on the splint, thus eliminating the need to use to preformed holes (Fig. 3A). The spin coating of SF solution onto the exterior of the splints imparted stiffness (but not rigidity), such that the splints recovered their shape after pressure was applied. The SF splints exhibited a loss in the maximum force as they degraded in protease solution at 37°C in a linear fashion with mass loss (Fig. 3B). A mass loss of 10% correlated to a loss in maximum force of approximately 30%. Evidence of degradation could also be observed in SEM images of the SF splints at 0 and 10% mass loss (Fig. 3Ci and 3Cii, respectively).

Rabbit Survival and Outcomes

The rabbits uniformly tolerated the tracheal splint implantation and immediate postoperative period well. Subcutaneous air collection was minimal, and the rubber band drain remained functional and in place for 24 to 48 hours. In all cases, the rabbit displaced or removed the rubber band prior to planned removal with cessation of subcutaneous air collection. Some of the animals had modest biphasic stridor noted with agitation (e.g., during toenail trimming or other semi-invasive routine ACF care). When stridor was present, the animals continued to breathe comfortably without respiratory distress. At all other times, the rabbits had quiet unlabored breathing throughout recovery. Wound healing was uncomplicated in all cases. None had weight loss, nor any other signs of distress or failure to thrive during the approximately 2 to 4 weeks of recovery.

Airway Measurements

In N = 3 controls, the average dynamic change in the area of the naïve rabbit trachea was 23% during spontaneous tidal respirations. Surgical resection of the anterior tracheal rings was effective at inducing tracheal collapse and modeling severe tracheomalacia, with a significant increase in the average change in airway area to 86% ($P < 0.001$). Immediately after splint implantation, the patency of the airway was improved and the average change in area decreased to 65%; however, it remained significantly higher than the change in area of the naïve trachea ($P < 0.001$). At the time of the first explantation (17 days postimplantation), patency was further improved and the change in airway area decreased to 47%, not significantly different than naïve trachea ($P = 0.18$). This trend continued with the remaining rabbits, which showed a 35% ($P = 0.83$) and 30% ($P = 0.98$) change in airway area at 24 and 31 days postimplantation, respectively (Fig. 4).

Tracheal Histology

Histopathology demonstrated a localized inflammatory process at the interface of the bioresorbable splint

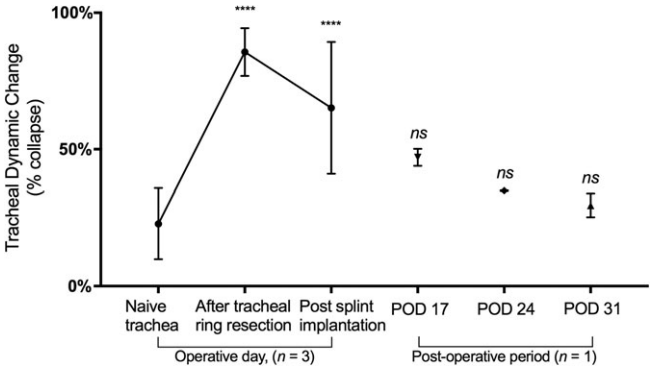

Fig. 4. Tracheal dynamic change as measured using an image-based assay. Surgically induced tracheomalacia resulted in a significant increase in dynamic change in airway caliber with tidal respirations. Subsequent splint placement reduced tracheal dynamic change to a level not statistically different from naïve trachea by POD 17 and persisted through POD 31.POD = postoperative day.

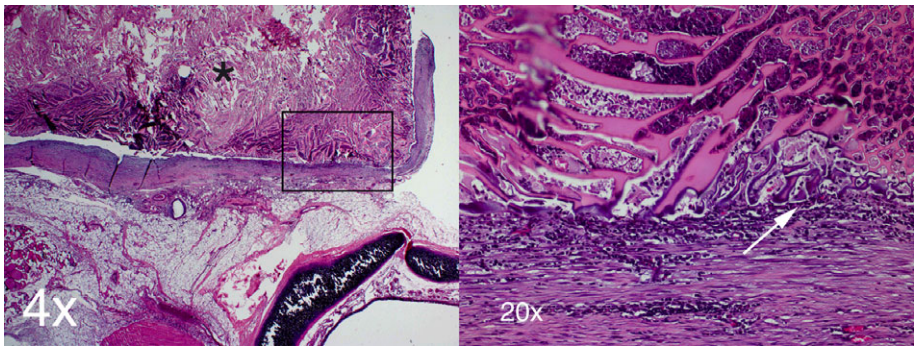

Fig. 5. Histology of resected rabbit trachea 24 days after implantation. At the 4 × magnification, the interface of the bioresorbable silk splint (identified with an asterisk) and underlying tracheal mucosa is well delineated. At the 20 × objective (corresponding to boxed area at 4×), a localized inflammatory reaction characterized by neutrophils, eosinophils, and mononuclear cells, with early signs suggestive of fibrosis, is evident (arrow). Neutrophils and cellular debris are also appreciated with the scaffold of the silk splint. [Color figure can be viewed in the online issue, which is available at www.laryngoscope.com.]

and tracheal mucosa, including apparent migration of neutrophils, eosinophils, and mononuclear cells to the site of the splint, with early signs suggestive of fibrosis localized at this interface (Fig. 5). Degradation of the silk splint was not observed and is not expected to occur within the time period studied. However, the presence of neutrophilic infiltration within the silk scaffold is suggestive of the early phase of biodegradation and resorption.

DISCUSSION

The anterior tracheal ring resection technique consistently produced significant airway malacia in our rabbit model. All three rabbits tolerated the procedure well, and neither respiratory distress nor other surgical complication was observed in the postoperative period. The image-based assay of dynamic change in airway area with spontaneous breaths provided a reliable and quantitative metric for tracheomalacia in our model, allowing us to quantify both the severity of the surgically induced malacia as well as the efficacy of the splint. This study, although relatively small, suggests that the current splint design yields a significant reduction in dynamic airway collapse in our model of severe malacia. Histology indicates an expected inflammatory response around the area of tissue injury at the site of the tracheal ring denudement from the underlying mucosa (Fig. 5). At the 24-day time-point, there is indication of fibrosis at the interface of the splint and tracheal submucosa, and evidence of cell infiltration into the scaffold. We hypothesize that this reactive fibrosis would subsequently lead to tissue integration with the splint matrix as the material breaks down, and that this is the principle mechanism for the progressive improvement in tracheal dynamics seen over time. A future larger study with longer follow-up could test this hypothesis.

We developed a two-step method to fabricate silk-based splints that exhibited both flexibility and stiffness. The silk splints were flexible such that when pressure was applied they could be manipulated without breaking, and they were able to conform to the tracheal wall. The splints were also stiff (but not rigid), in that they resisted deformation when pressure was applied, providing radial strength to the weakened tracheal wall. The fabrication method developed here is advantageous in that will allow us to modulate the stiffness and degradation rate of the implants to meet future clinical needs. Stiffness and degradation rate can be modified by changing the secondary structure of the silk protein, the concentration of the silk protein, the porosity of the splint, or the thickness of the silk coating.

Through an in vitro degradation assay, we were able to relate mass loss to a loss in force and demonstrate that this relationship was linear. In future longitudinal studies, in vivo degradation estimated from histological images or the change in weight of explanted splints could be compared to the in vitro degradation data to estimate the change in mechanical properties. Degradation in vivo was not observed over the time period in the present study. Degradation rate has been shown to be dependent on the silk protein concentration, secondary structure, material density, and the in vivo location of the implant.[20,23] Although no previous preclinical studies exist that could be used as a direct comparison to this work in terms of silk scaffold processing, animal model, and implant location, studies carried out under similar conditions suggest that degradation may become evident after 4 to 6 months and appear more significantly after 12 months.[26–28]

CONCLUSION

We report a resorbable SF-based splint for the treatment of pediatric airway collapse. Severe tracheomalacia is a serious condition and is not infrequent, accounting for almost half of all cases. External splints have been reported in both preclinical and human use, although these have been from nondegradable materials or degradable materials used off-label and have not been developed in the context of the pediatric airway. This in vivo pilot study in a rabbit model of surgically induced severe tracheomalacia suggests good efficacy from the silk splint, with minimal adverse effects and no mortality prior to the planned end of the experiment. Moving forward, we will further validate this implant in the rabbit model of tracheomalacia, including more distal time-points to fully

characterize the degradation kinetics in vivo and ensure the persistence of efficacy in terms of airway patency over time. As noted, the fabrication method of the silk splint will allow us to modulate the degradation rate and stiffness, showing substantial promise in future work. Additionally, we plan to explore splint efficacy in a model of posttracheostomy laryngotracheal reconstruction.

ACKNOWLEDGMENTS

The authors would like to acknowledge the assistance of the MEEI Animal Care Center, in particular Mrs. Stephanie Ventura, whose technical expertise made the in vivo aspects of this project possible. We gratefully acknowledge the assistance of Ms. Patricia Della Pelle and Dr. Ivy A. Rosales of the Massachusetts General Hospital Immunopathology Research Lab in the preparation and interpretation of tracheal histology images. And we gratefully recognize Dr. Kishore Sandu for sharing his excellent techniques for this preclinical model. We also thank the National Institutes of Health (R01AR068048) and the Hartnick Research Fund for support of this work.

BIBLIOGRAPHY

1. Carden KA, Boiselle PM, Waltz DA, Ernst A. Tracheomalacia and tracheobronchomalacia in children and adults. *Chest* 2005;127:984–1005.
2. Boogaard R, Huijsmans SH, Pijnenburg MWH, Tiddens HAWM, de Jongste JC, Merkus PJFM. Tracheomalacia and bronchomalacia in children. *Chest* 2005;128:3391–3397.
3. Masters IB, Chang AB. Interventions for primary (intrinsic) tracheomalacia in children. In: Masters IB, ed. *Cochrane Database of Systematic Reviews*. Vol 131. Chichester, UK: John Wiley & Sons, Ltd; 2005:66.
4. Hysinger EB, Panitch HB. Paediatric tracheomalacia. *Paediatr Respir Rev* 2016;17:9–15.
5. Deacon JWF, Widger J, Soma MA. Paediatric tracheomalacia: a review of clinical features and comparison of diagnostic imaging techniques. *Int J Pediatr Otorhinolaryngol* 2017;98:75–81.
6. Hoetzenecker K, Schweiger T, Denk-Linnert DM, Klepetko W. Pediatric airway surgery. *J Thorac Dis* 2017;9:1663–1671.
7. Ho AS, Koltai PJ. Pediatric tracheal stenosis. *Otolaryngol Clin North Am* 2008;41:999–1021.
8. Valerie EP, Durrant AC, Forte V, Wales P, Chait P, Kim PCW. A decade of using intraluminal tracheal/bronchial stents in the management of tracheomalacia and/or bronchomalacia: is it better than aortopexy? *J Pediatr Surg* 2005;40:904–907.
9. Johnston MR, Loeber N, Hillyer P, Stephenson LW, Edmunds LH. External stent for repair of secondary tracheomalacia. *Ann Thorac Surg* 1980;30: 291–296.
10. Ando M, Nagase Y, Hasegawa H, Takahashi Y. External stenting: a reliable technique to relieve airway obstruction in small children. *J Thorac Cardiovasc Surg* 2017;153:1167–1177.
11. Morrison RJ, Sengupta S, Flanangan CL, Ohye RG, Hollister SJ, Green GE. Treatment of severe acquired tracheomalacia with a patient-specific, 3D-printed, permanent tracheal splint. *JAMA Otolaryngol Neck Surg* 2017;143:523.
12. Zopf DA, Flanagan CL, Wheeler M, Hollister SJ, Green GE. Treatment of severe porcine tracheomalacia with a 3-dimensionally printed, bioresorbable, external airway splint. *JAMA Otolaryngol Neck Surg* 2014;140:66.
13. Zopf DA, Hollister SJ, Nelson ME, Ohye RG, Green GE. Bioresorbable airway splint created with a three-dimensional printer. *N Engl J Med* 2013; 368:2043–2045.
14. Gorostidi F, Courbon C, Burki M, Reinhard A, Sandu K. Extraluminal biodegradable splint to treat upper airway anterior malacia: a preclinical proof of principle. *Laryngoscope* 2018;128:E53–E58.
15. Willner A, Saul. Extraluminal laryngotracheal fixation with absorbable miniplates. *Arch Otolaryngol Head Neck Surg* 1995;121:1356–1360.
16. Robey TC, Eiselt PM, Murphy HS, Mooney DJ, Weatherly RA. Biodegradable external tracheal stents and their use in a rabbit tracheal reconstruction model. *Laryngoscope* 2000;110:1936–1942.
17. Bowe SN, Colaianni CA, Hartnick CJ. Management of severe suprastomal collapse with bioabsorbable microplates. *Laryngoscope* 2017;127: 2823–2826.
18. Gorostidi F, Reinhard A, Monnier P, Sandu K. External bioresorbable airway rigidification to treat refractory localized tracheomalacia. *Laryngoscope* 2016;126:2605–2610.
19. Javia LR, Zur KB. Laryngotracheal reconstruction with resorbable microplate buttressing. *Laryngoscope* 2012;122:920–924.
20. Thurber AE, Omenetto FG, Kaplan DL. In vivo bioresponses to silk proteins. *Biomaterials* 2015;71:145–157.
21. Lovett M, Cannizzaro C, Daheron L, Messmer B, Vunjak-Novakovic G, Kaplan DL. Silk fibroin microtubes for blood vessel engineering. *Biomaterials* 2007;28:5271–5279.
22. Tsioris K, Raja WK, Pritchard EM, Panilaitis B, Kaplan DL, Omenetto FG. Fabrication of silk microneedles for controlled-release drug delivery. *Adv Funct Mater* 2012;22:330–335.
23. Altman GH, Diaz F, Jakuba C, et al. Silk-based biomaterials. *Biomaterials* 2003;24:401–416.
24. Lee KS, Sun MRM, Ernst A, Feller-Kopman D, Majid A, Boiselle PM. Comparison of dynamic expiratory CT with bronchoscopy for diagnosing airway malacia. *Chest* 2007;131:758–764.
25. Lee EY, Boiselle PM. Tracheobronchomalacia in infants and children: multidetector CT evaluation. *Radiology* 2009;252:7–22.
26. Wang Y, Rudym DD, Walsh A, et al. In vivo degradation of three-dimensional silk fibroin scaffolds. *Biomaterials* 2008;29:3415–3428.
27. Uebersax L, Apfel T, Nuss KMR, et al. Biocompatibility and osteoconduction of macroporous silk fibroin implants in cortical defects in sheep. *Eur J Pharm Biopharm* 2013;85:107–118.
28. Fan H, Liu H, Wong EJW, Toh SL, Goh JCH. In vivo study of anterior cruciate ligament regeneration using mesenchymal stem cells and silk scaffold. *Biomaterials* 2008;29:3324–3337.